Kinetic Methods. (a) Potentiometric Titration. Solutions (90% aqueous DMF, v/v) of TPP and the sulfone were made such that addition of 10 ml of sulfone solution to the TPP solution gave solutions that were 0.100 *M* in TPP and 0.0100 *M* in sulfone. The solutions were mixed at the appropriate reaction temperature and the time at mixing was taken as time zero. Samples (*ca.* 5 ml) were withdrawn with a 5-ml pipet fitted with a three-way stopcock. For reactions run at $\geq 60°$ and for all the α-iodo sulfones, individual aliquots were placed in sealed ampoules. The ampoules for the α-iodo sulfones were wrapped with aluminum foil. The aliquots were quenched with 40 ml of distilled deionized water and the solution filtered through Johns–Manville Celite, analytical filter aid. The filtrate was titrated against silver nitrate solution on a Sargent-Welch Recording Titrator Model D. Rate constants were determined from plots of log $(D_\infty - D_t)$ *vs.* time, where *D* is the distance to the point of inflection. The second-order rate constants were determined by dividing the pseudo-first-order rate constants by the concentration of TPP. The TPP concentration was varied from 0.10 to 0.40 *M*, and the sulfone concentration was varied from 0.010 to 0.001 *M*, and in each case the rate plots exhibited a first-order pattern.

(b) Conductiometric Technique. Separate solutions of TPP and sulfone were placed in a constant-temperature bath and allowed to equilibrate for 30 min. The solutions were mixed and placed into a Freas conductivity cell which was thermostated in the same constant-temperature bath. The timer was started and conductance readings were taken at various intervals with a Barnstead Conductivity Bridge, Model PM-70CB. The rate constants were obtained by plotting log $(C_\infty - C_t)$ *vs.* time, where *C* is the conductance reading in mhos. The second-order rate constants were obtained by dividing the pseudo-first-order rate constants by the concentration of TPP. The TPP concentrations were 0.10–0.20 *M*, and the sulfone concentration was 0.0010 *M*.

(c) Spectrophotometric Technique. A solution of TPP containing chlorophenol red indicator (Eastman) was made such that the absorbance at 599.4 nm was *ca.* 0.8. Three milliliters of this solution in a cuvet was thermostated in the cell holder of a Cary 15 ultraviolet–visible spectrophotometer. To this solution was added 10 μl of sulfone solution and absorption as a function of time was recorded. The TPP concentration varied from 0.00010 to 0.200 *M* and the sulfone concentration varied from 1.50×10^{-5} to 7.50×10^{-6} *M*. The rate constants were obtained by dividing the pseudo-first-order rate constants by the concentration of TPP.

Comparison of Kinetic Methods. The second-order rate constants were determined for α-bromo-*m*-cyanobenzyl phenyl sulfone (**3d**) by all three techniques which gave the following data.

Method	Temp, °C	10^3k, M^{-1} sec^{-1}
a	19.98	1.65 ± 0.10
c	19.98	1.50 ± 0.06
b	50.19	12.2 ± 0.82
c	50.19	11.4 ± 0.65

Product Analysis. Preparative runs for these reactions were made with **2f**, **3b**, and **5a** at temperatures of 70–80° for a reaction time of 1 half-life. Upon work-up, each reaction mixture yielded a solution which was shown by nmr spectroscopy to be a 50:50 mixture of starting α-halo sulfone and reduced sulfone (**6**). The sulfones were isolated by preparative tlc (silica gel, methylene chloride) and identified by ir, melting point, and mixture melting point.

Acknowledgments. We wish to thank the National Science Foundation for their generous support of this work under Grant No. GP-29497. The kinetic data for **11** and the deuterium isotope effect measurements were determined by R. L. Harper. Support from the University of Maryland Computer Science Center also is acknowledged.

Interpretation of the Charge and Energy Changes in Two Nucleophilic Displacement Reactions

R. F. W. Bader,* A. J. Duke, and R. R. Messer

Contribution from the Department of Chemistry, McMaster University, Hamilton, Ontario L8S 4M1, Canada. *Received June 22, 1973*

Abstract: By means of the virial partitioning method the energies of activation for two SN2 displacement reactions (F^- and CN^- + CH_3F) are divided into contributions from spatially defined fragments of the total system. In this way, the course of a reaction may be followed for each fragment individually, by monitoring the change in its charge distribution and kinetic energy from reactants to transition state to products. The bound (F) fragment of CH_3F, for example, is more stable than an isolated F^- ion by −199 kcal/mol. In the FCH_3CN^- transition state the net charge on the (leaving) fluorine fragment has developed to −0.954 e and its energy increased to within 36 kcal/mol of F^-. The process of bond breaking with the leaving group thus contributes 163 kcal/mol to a total activation energy of 22 kcal/mol. In general, it is found that the nucleophilic fragments (F) and (CN) and the (C) fragment of CH_3F are stabilized in the formation of the transition state, while the leaving (F) fragment is considerably destabilized. The (H) fragments are raised in energy (by ~15 kcal/mol) because of the compression of these fragments in both transition states. This compression of the (H) fragments results in a transfer of electronic charge density from (H) to (C). The (C) fragment bears a net positive charge in both transition states (+0.463 e in FCH_3F^- and +0.316 e in FCH_3CN^-).

This paper presents a detailed study of the redistribution of the charge density and the associated energy changes for two gas-phase nucleophilic displacement reactions. The reactions considered are the displacement of fluoride ion from methyl fluoride by fluoride ion and by cyanide ion. The changes in the charge distribution and energy during the course of each reaction are related to one another *via* the virial partitioning method. This is a procedure for spatially subdividing a system into fragments wherein the kinetic and potential energies of each fragment obey the virial relationship.[1,2] The partitioning surfaces

(1) R. F. W. Bader and P. M. Beddall, *J. Chem. Phys.*, **56**, 3320 (1972).

(2) R. F. W. Bader, P. M. Beddall, and J. Peslak, Jr., *J. Chem. Phys.*, **58**, 557 (1973).

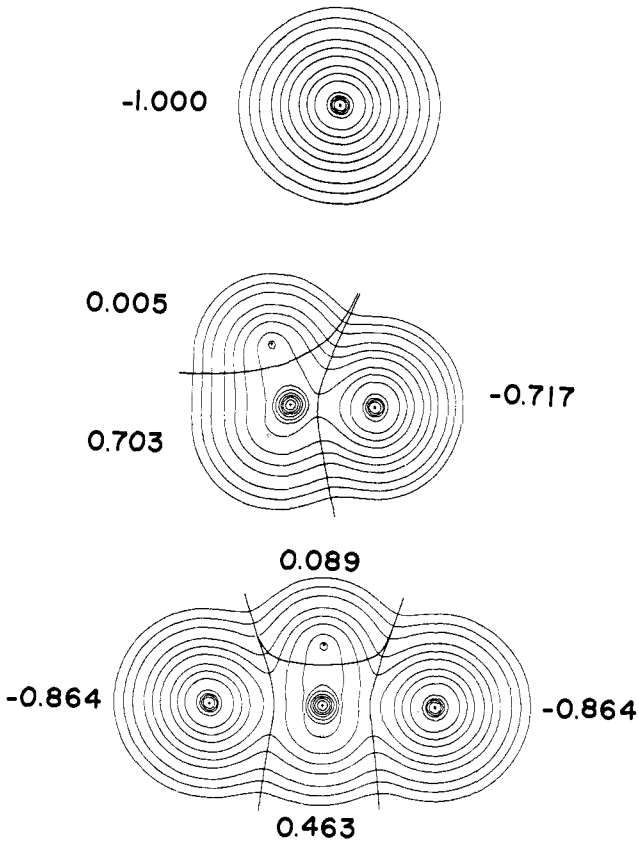

Figure 1. Contour diagrams of the electronic charge density in F^-, CH_3F, and the transition state FCH_3F^- showing the virial partitioning surfaces for and the net charges on each fragment. The contours in this figure and Figure 2 (in au) increase in value from the outermost contour inward in steps of 2×10^n, 4×10^n, and 8×10^n. The smallest contour value is 0.002 with n increasing in steps of unity to yield a maximum contour value of 20.

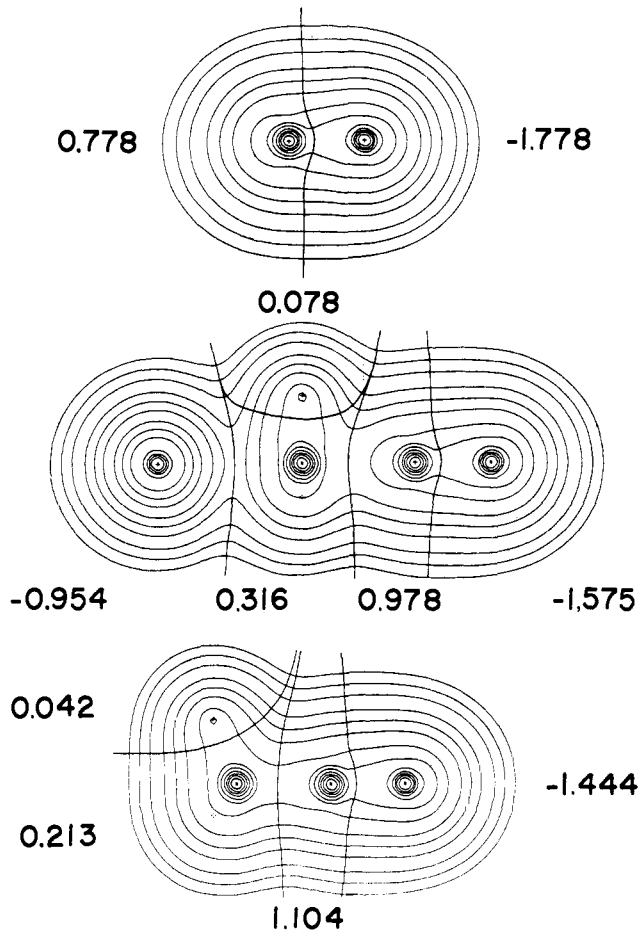

Figure 2. Contour diagrams of the electronic charge density in CN^-, the transition state FCH_3CN^- and CH_3CN showing the virial partitioning surfaces for and net charges on each fragment.

defining the fragments are determined by the minima in the charge distribution encompassing each nucleus. As the reaction proceeds and the topography of the charge distribution changes, the boundary surface of each fragment undergoes a continuous change, as does its total electron population and energy. However, at each stage of the reaction, the kinetic energy of a given fragment must equal minus one-half of the virial of all the forces exerted on the charge density of the fragment. Thus, by means of this virial restraint, we may partition a total energy change into energy changes for each fragment of the system and simultaneously relate these changes to the redistribution of charge in each fragment.

In particular, the energy of activation may be partitioned into the separate energy changes experienced by the nucleophile (F^- or CN^-), the leaving group (F^-), and the carbon and hydrogen fragments of the substrate CH_3F.

The partitioning surface is defined by that collection of gradient paths defined by the vectors $\nabla\rho(\mathbf{x})$ which pass through the null point $\nabla\rho(\mathbf{x}) = 0$ between a pair of adjacent nuclear centers and terminate at another null point, generally at infinity. It is a property of the vector $\nabla\rho(\mathbf{x})$ that it be normal to contour lines of constant density. In the present examples, an internuclear null point in $\nabla\rho(\mathbf{x})$ corresponds to a saddle point in the charge distribution.[3] Such surfaces, termed zero-flux surfaces, are illustrated in Figures 1 and 2 for the reactants and transition states. They are unique in that only one such surface contains a given internuclear null point. for all gradient paths not passing through a null point terminate at a nucleus.

It has been demonstrated that a fragment bounded by a zero-flux surface $S(\mathbf{x})$, one satisfying the relationship

$$d\rho(\mathbf{x})/d\bar{n} = 0, \qquad \mathbf{x} \in S(\mathbf{x}) \tag{1}$$

(where $\bar{\mathbf{n}}$ is the vector normal to $S(\mathbf{x})$ at each $\mathbf{x}$), has a well-defined kinetic energy. In addition, it has been demonstrated that the kinetic energy of such a fragment satisfies the virial relationships.[1,2] That is, for a fragment (A)[4]

$$-2\bar{T}(A) = \bar{V}'(A) + \bar{V}''(A) + \bar{V}_n(A) \equiv \bar{V}(A) \tag{2}$$

where $\bar{T}(A)$ is the kinetic energy of (A), $\bar{V}'(A)$ is the attractive interaction of the charge density in (A) with all of the nuclei in the system, and $\bar{V}''(A)$ is the self-repulsion of the electrons in (A) and one-half of the

(3) For further details on the properties and determination of the partitioning surfaces and the nuclear virial contribution in polyatomic systems see G. Runtz, Ph.D. Thesis, McMaster University, 1973. A null point in $\nabla\rho(\mathbf{x})$ does not necessarily lie on an internuclear axis (*e.g.*, $\nabla\rho(\mathbf{x}) = 0$ lies off the C–H axis in CH_3F) unless the axis is a symmetry axis (*e.g.*, $\nabla\rho(\mathbf{x}) = 0$ is on the C–F axis in CH_3F).

(4) R. F. W. Bader and P. M. Beddall, *J. Amer. Chem. Soc.*, **95**, 305 (1973). This paper provides a detailed summary of the contributions to the total virial of a fragment.

repulsion of the electrons in (A) with all the remaining electrons in the system.[2] The total nuclear virial $\bar{V}_n$ is equal to the sum of the nuclear repulsive interactions within the system plus the virial of the external forces acting on the nuclei when they are not at their equilibrium positions. The sum of the nuclear and external forces is equal and opposite to the forces exerted on the nuclei by the charge distribution as calculated by the Hellmann–Feynman theorem. Thus, the nuclear virial contribution for a fragment (A) is determined by the fraction of the total electron–nuclear force which is generated by the charge distribution in fragment (A) multiplied by its appropriate position vector.[3] When there are no external forces acting on the nuclei, the nuclear virial for the total system and for each fragment reduces to just the nuclear–nuclear repulsive contribution. In this case, the further virial relationship is

$$-\bar{T}(\mathrm{A}) = \bar{E}(\mathrm{A}) \tag{3}$$

where $E(\mathrm{A})$ is the total energy of fragment (A).

Energy *changes* may be partitioned similarly for each fragment, *i.e.*

$$-2\Delta\bar{T}(\mathrm{A}) = \Delta\bar{V}'(\mathrm{A}) + \Delta\bar{V}''(\mathrm{A}) + \Delta\bar{V}_n(\mathrm{A}) \equiv \Delta\bar{V}(\mathrm{A}) \tag{4}$$

$$-\Delta\bar{T}(\mathrm{A}) = \Delta\bar{E}(\mathrm{A}) \tag{5}$$

Thus, the increase or decrease in the stability of a fragment for any change in the system may be determined from the sign of $\Delta\bar{T}(\mathrm{A})$ in eq 5. If $\Delta\bar{T}(\mathrm{A}) > 0$, then $\Delta\bar{E}(\mathrm{A}) < 0$ and the fragment has increased in stability as a result of the change. If $\Delta\bar{T}(\mathrm{A}) < 0$, $\Delta\bar{E}(\mathrm{A}) > 0$ and the fragment is destabilized by the change in the system. Equation 4 relates the change in $\Delta\bar{T}(\mathrm{A})$ to the change in the total virial of the fragment and allows one to relate the change in the stability of the fragment to the changes in the individual potential energy contributions. This approach has been previously applied to the charge redistributions and energy changes associated with the formation of the first-row diatomic hydrides.[4]

The present results were obtained from wave functions, previously determined in this laboratory,[5] which describe the minimum potential energy surfaces for the reactions

$$CH_3F + F^- \longrightarrow CH_3F + F^- \tag{6}$$

and

$$CH_3F + CN^- \longrightarrow CH_3CN + F^- \tag{7}$$

The wave functions are close to the Hartree–Fock limit and represent the best single-determinant calculations carried out so far for SN2 type reactions in terms of basis set size and absolute energies. The reader is referred to ref 5 for details of the calculation. We report here only the required results of the calculations.

Careful geometry optimizations were performed for all the reactants and products and for various points along the reaction coordinates. In general, the calculated and experimental bond lengths and bond angles for CH_3F and CH_3CN differed by no more than 0.02 Å and 0.8°, respectively. The symmetrical (D_{3h} geometry) configuration of FCH_3F^- with a C–F bond length of 3.586 au was found to yield the maximum energy on the minimum energy path for the displacement reaction, yielding an activation energy of 7.26 kcal/mol.[6] In general, our results for reaction (6) are in good general agreement with those of Dedieu and Veillard[7] who studied this and three other SN2 type displacements using a slightly smaller basis set. For example, their calculated energy of activation for reaction (6) was 7.9 kcal/mol. Their paper provides a thorough view of the variation in the total energies along the reaction paths.

An asymmetric geometry corresponding to a point on the minimum energy path and occurring just before (or just after) the symmetrical transition state possesses an energy 6.09 kcal/mol above that of the reactants with C–F bond lengths of 3.636 and 3.380 au and an FCH bond angle of 86.88°. A comparison of this asymmetric geometry with that of the transition state indicates that as the nucleophilic fluorine decreases its distance of approach by 0.050 au, the leaving fluorine increases its separation by 0.206 au. Thus, the leaving (F) remains relatively tightly bound until the nucleophilic (F) has approached to a distance close to its transition-state value. Further approach by the nucleophilic (F) then causes a relatively large increase in the separation of the leaving (F). A similar result was obtained by Dedieu and Veillard.[7]

Because of the large number of basis functions required to yield a theoretical description of the species FCH_3CN^- equivalent to that obtained for FCH_3F^-, only the F–C and C–CN bond lengths were optimized to fix the transition-state geometry in reaction (7). The C–N bond length was taken to be that of the ion, the C–H distance was that found for FCH_3F^-, and the methyl group was assumed to be planar. With these restrictions the activation energy for reaction (7) is found to be 22.6 kcal/mol. The transition state has a very extended C–F bond length, 4.225 au compared with 2.650 au in CH_3F, and a C–CN bond length of 3.280 au compared with a value of 2.766 au in the product CH_3CN.

Virial Partitioning

The significance of virial partitioning is based upon the following observations.[1,2,8] The extent to which the properties of a fragment are additive between different systems is determined by the extent to which the charge distribution of the fragment is unchanged between the systems. As a consequence of the definition of the fragment boundaries, the differences between the charge distributions of a given fragment in different systems are minimized. Thus, the virial partitioning method yields chemically identifiable fragments by maximizing the retention of the distribution of charge and hence of the properties for each fragment between different systems. When one observes additivity of properties experimentally, this is reflected in the constancy of the charge distribution of the fragments as defined here. On the other hand, when additivity of properties is not found, the fragments and their properties are found to exhibit changes to a corresponding degree.

(5) R. F. W. Bader and A. J. Duke, *Chem. Phys. Lett.*, 10, 631 (1971).

(6) The addition of a second set of d functions for all centers other than H to the basis set employed in the description of reaction 6 changed the value of the activation energy to 7.14 kcal/mol, a change of only 1.7%.

(7) A. Dedieu and A. Veillard, *J. Amer. Chem. Soc.*, **94**, 6730 (1972).

(8) R. F. W. Bader and P. M. Beddall, *Chem. Phys. Lett.*, **8**, 29 (1971).

Table I. Fluorine Fragment Kinetic Energies and Virial Contributions Relative to F^- Ion

(F)	r(C–F), au	N(F)	ΔT(F), kcal/mol	$\Delta V'$(F),[a] au	$\Delta V''$(F), au	ΔV_n(F),[b] au
$CH_3(F)$	2.650	9.717	199	−29.721	12.440	16.647
$FCH_3(F)^-$	3.586	9.864	60	−35.835	17.253	18.391
$NCCH_3(F)^-$	4.255	9.954	36	−35.621	17.473	18.033

[a] 1 au of energy = 627.71 kcal/mol. [b] In general, LCAO–MO–SCF wave functions, even those close to the Hartree–Fock limit, do not exactly satisfy the Hellmann–Feynman theorem. Primarily because of the errors in the Hellmann–Feynman forces and hence in $\bar{V}_n$ such functions exhibit errors in the virial relationship for the total molecule.[1,2] For the purpose of discussing energy changes the errors in $\bar{V}_n$ are ignored and the values of $\Delta\bar{V}_n$ given in Tables I and II are such that they satisfy the fragment virial relationship exactly.

We have also found that the charge distribution of a fragment is determined by the virial of all the forces exerted on it.[1,2] To the extent that the total virial of a fragment remains unchanged in two different systems, regardless of the changes in the individual force contributions to the virial, the charge density and the properties of the fragment remain unaltered. Since each fragment obeys the virial relationship, any change in its virial and the energetic consequences of the accompanying change in its charge distribution are quantitatively determined by the change in its kinetic energy.

If one views (Figures 1 and 2) the (F) fragment in CH_3F and in the two transition states one sees a progressive change in the charge distribution of the fragment toward that of the isolated F^- ion. Since it is the charge density which is the carrier of the information for all the properties of the system, the extent of the reaction for any fragment at any point along the reaction coordinate is determined by observing the extent to which the charge density of the fragment has approached the distribution found in the product fragment. This comparison is made quantitative by monitoring the kinetic energy of the fragment. When the kinetic energy difference between the reactant fragment and its product form vanishes, the reaction is complete.

Table I lists the population N(F), the kinetic energy, and the three potential contributions to the virial (see eq 4) for the leaving (F) fragment in CH_3F and the two transition states, all relative to those of a free F^- ion. We first note that while the individual contributions to the virial of the bound (F) differ from those of the free F^- ion by 1×10^4–3×10^4 kcal/mol, the total virials and hence the kinetic energies differ by amounts of normal chemical magnitude. Thus, in spite of the radically different individual forces exerted on bound (F) relative to F^-, one may still chemically identify a fluorine because of the relatively small differences in their charge distributions as determined by the correspondingly small differences in their *total* virials. The bound (F) in CH_3F possesses a kinetic energy 199 kcal/mol greater than that of F^-, and, since the CH_3F is in its equilibrium geometry, we may apply eq 5 and state that this bound (F) is more stable in terms of its total energy than the isolated F^- by a corresponding amount. As the separation of the bound (F) increases, its total charge and kinetic energy approach those of the isolated F^- ion, changes which parallel the progressive change in its charge distribution toward the same limit.

It is clear from the preceding discussion that the virial partitioning of molecular energies requires that one view energies and changes in energies from a point of view which is different from the usual one. In general, the virial partitioning surfaces bisect what are normally considered to be chemical bonds. Thus, rather than referring to the energy required to break or form a bond (a concept which has a rigorous meaning only in a diatomic system) one instead refers to the changes in energy of the individual fragments, where any one fragment may be bonded to one or more other fragments. For example, we calculate the reaction

$$CH_3F + CN^- \longrightarrow CH_3CN + F^-$$

to be endothermic by ~5 kcal/mol. The (F) fragment in CH_3F is 199 kcal/mol more stable than is an isolated F^- ion and thus the formation of this ion contributes a corresponding amount to the energy of reaction. The CN^- ion, on the other hand, is stabilized by *ca.* −77 kcal/mol when transformed into the bound (CN) fragment of CH_3CN. The (CH_3) fragment undergoes a significant stabilization in this exchange reaction, being more stable when bound to (CN) than to (F) by *ca.* −117 kcal/mol. These separate energy changes may in turn be related to the redistribution of charge density in each fragment, as illustrated below.

In an isolated, closed-shell, mononuclear system the charge distribution is spherical and centered on the nucleus, indicating that it is governed by a single nuclear center of force. The extent to which this pattern for the charge distribution is approached for a fragment in a molecule is an indication of the extent to which the charge density is governed primarily by the forces originating within the fragment as opposed to the forces exerted on it by neighboring fragments, forces which tend to distort it from the spherical pattern. In the systems under consideration here (Figures 1 and 2), the charge distributions of the (F) fragments approach this limiting, isolated behavior most closely. This is the charge density representation of the statement that fluorine is the most electronegative of the elements H, C, N, and F. The contours of (F) which cross the boundary surface between this fragment and (C) exhibit a distinct "pinched" effect. The central field potentials exerted on the charge density in (H) and on the valence charge density of (C) are more evenly matched (C and H have nearly equal electronegativities), and this is reflected in the even distribution of the valence charge density over the boundary surface between the (C) and (H) fragments.

The net charge (C(A) = $Z_A - \bar{N}$(A), where Z_A is the nuclear charge and $\bar{N}$(A) the electron population of (A)[4]) on each fragment is indicated in Figures 1 and 2. A bound (F) fragment is generally characterized by a large net negative charge, with a large central force exerted on its charge distribution. For example, the net charge on (F) varies monotonically from −0.94

to −0.44 across the period from LiF to NF, with a value of −0.78 in CF (× $^2\Pi$). The null point ($\nabla\rho(\mathbf{x}) = 0$) for (C) bonded to (N), (O), or (F) occurs at ~0.75 ± 0.03 au on the bonded side of the carbon nucleus. Thus, the (C) fragment, when in combination with a more electronegative fragment, has a relatively small bonded radius and consequently a relatively large net positive charge.

Description of the Transition States

Table II lists the changes in the net charges on each fragment incurred on passage to the transition state. The C–F bond length increases by 0.936 au from its value in CH_3F to 3.586 au in the symmetrical $(FCH_3F)^-$ transition state and the net charge on both F fragments is −0.864 e. The net charge on (CH_3) changes very little, the charge lost by the nucleophilic F^- being almost equal to the charge gained by the leaving (F). In the $NCCH_3F^-$ transition state, the C–F bond length has increased by 1.575 au to 4.225 au and the net charge on (F) has increased to −0.954 e. The incipient formation of F^- is evident in the transition states, particularly in the CN^- displacement.[9] The CN^- approaches to within 0.514 au of its final equilibrium C–C bond length of 2.766 au in CH_3CN. The CN^- transfers 0.168 e to (CH_3) and 0.237 e to (F) in the formation of the transition state, the (C) and (N) fragments contributing nearly equal amounts of 0.2 e each.

Table II. Kinetic and Potential Energies of Activation and Population Changes for Fragments

(A)	$\Delta C(A)$[a]	$\Delta T(A) = -\Delta E(A)$, kcal/mol	$\Delta V'(A)$,[b] au	$\Delta V''(A)$, au	$\Delta V_n(A)$, au
		$CH_3F + F^-$			
(C)	−0.240	+117	−12.013	6.315	5.326
(H)	+0.084	−15	−1.320	0.777	0.591
(CH_3)	+0.012	+72	−15.974	8.646	7.101
(F)	−0.147	−139	−6.114	4.814	1.743
(F^-)	+0.136	+60	−35.835	17.253	18.390
		$CH_3F + CN^-$			
(C)	−0.387	+164	−14.813	7.604	6.687
(H)	+0.073	−15	−1.690	0.945	0.792
(CH_3)	−0.168	+119	−19.883	10.438	9.063
(F)	−0.237	−163	−5.900	5.034	1.384
(CN^-)	+0.403	+22	−41.011	19.575	21.366
(C)	+0.200	+97	−20.208	9.592	10.308
(N)	+0.203	−75	−20.803	9.983	11.058

[a] $\Delta C(A) = C(A, \text{transition state}) - C(A, \text{reactant})$. A negative $\Delta C(A)$ implies an increase in the electron population. [b] 1 au of energy = 627.71 kcal/mol.

While CH_3 bears a net positive charge in both transition states, its value is reduced from that in CH_3F in the CN^- reaction and increased slightly in the F^- case. In both cases, however, the net charge on just the (C) fragment of (CH_3) is reduced from its initial value in CH_3F because of a substantial transfer of charge from (H) to (C). The absolute extent of this charge transfer in CH_2F is negligible, with $C(H) = +0.005$. In FCH_3F^- the net charge on (H) has increased to +0.089 e and in $NCCH_3F^-$ to +0.078 e. In the product CH_3CN, the transfer from (H) to (C) is intermediate, the net charge on (H) being +0.042 e.

These changes in the net populations of the (H) fragments in the above molecules (and others referred to below) are of interest in that they correlate with previous rationalizations based on the "hyperconjugative" mechanism of electron release. It is at first surprising that there is little donation of charge from (H) to (C) in CH_3F where there is a large net positive charge on the (CH_3) fragment, while in CH_3CN there is a significant transfer from (H) to (C) in spite of the fact that the net charge on (CH_3) is reduced relative to its value in CH_3F, because of the transfer of charge from (CN). Observations of a similar nature apply to the transfer of charge from (H) to (B) in (BH_3) when BH_3 acts as a Lewis acid.[3] The population of (H) increases relative to (H) in BH_3, in the formation of BH_3F^-, but decreases by 0.072 e in the formation of BH_3CO. We have previously observed that the greater the transfer of charge from A → B in AB, the greater is the degree of polarization of the π density on B toward A.[10] This back transfer occurs from (F) toward (C) in CH_3F and from (F) toward (B) in BH_3F^- but not from (C) of (CN) toward (C) of (CH_3) in CH_3CN or from (C) of (CO) to (B) in BH_3CO. (The (C) fragments of (CN) and (CO) have net positive charges of +1.104 and +1.179, respectively.) Thus, the release of electrons from (H) → (C) in (CH_3) and from (H) → (B) in (BH_3) occurs to a significant degree when the (C) or (B) fragments are joined to a net positively charged fragment, but not when neighboring a net negatively charged fragment in normal molecules. These observations agree with the findings of Pople and Beveridge based on their method of population analysis.[11]

That the (H) fragments donate charge to (C) in the two transition states considered here is apparently at variance with the above generalization. This appears to be particularly so for FCH_3F^- where (C) is bonded linearly to two negatively charged (F) fragments. This result is best explained as a result of "crowding" of the (H) fragments in the transition state. From Figure 1 it is clear that the presence of the two (F) fragments in the transition state, each of expanded size because of their increased charge relative to (F) of CH_3F, reduces the effective volume of space occupied by the (H) fragments. An integration of the (H) fragment volumes out to the outermost contour illustrated in the figure indicates that the volume occupied by the charge distribution of the (H) fragment is decreased by 12% in the formation of the FCH_3F^- transition state. The same decrease in the spatial extent of the (H) charge distribution is evident in the $NCCH_3F^-$ transition state. The nonbonded radius of (H) (the distance from the proton to the 0.002 au contour on its nonbonded side along the C–H bond axis) is of the same value, ~2.2 au in CH_3F and both transition states. The bonded radius of (H) (the distance from the proton to the density minimum along the C–H bond axis), on the other hand, decreases from

(9) Note the increase in the number of closed contours which encircle only the fluorine nucleus for (F) in CH_3F, FCH_3F^-, and FCH_3CN^-. The values of $\rho(\mathbf{x})$ at the internuclear null points on the boundary of (C) and (F) for the above species are 0.221, 0.063, and 0.031 au, respectively. The corresponding values of $\rho(\mathbf{x})$ on the boundary of (C) of CH_3 and (C) of CN are 0.270 au in CH_3CN and 0.137 au in the transition state.

(10) R. F. W. Bader, I. Keaveny, and P. E. Cade, *J. Chem. Phys.*, 47, 3381 (1967).

(11) J. A. Pople and D. L. Beveridge, "Approximate Molecular Orbital Theory," McGraw-Hill, New York, N. Y., 1970, p 119 ff.

0.73 au in CH_3F to ~0.67 au in the transition states, an indication of the migration of charge from (H) to (C). Thus, it is energetically more favorable for a compressed (H) fragment to transfer charge out of the fragment and into a neighboring system rather than transfer it to its nonbonded region, a region of relatively high potential.

As discussed below, each (H) fragment is destabilized by ~15 kcal/mol in the transition state relative to CH_3F, a result of the increase in the electron–electron and nuclear repulsion forces exceeding the increase in the nuclear–electron attractive interactions in the attainment of the transition state. Clearly, if an (H) fragment is compressed and raised in energy in a pentavalent carbon system, then, as is recognized, effects well characterized by the term steric play an important role in the energetics of the formation of the transition state in an SN2 displacement.

In summary, the (C) bears a substantial net positive charge in both transition states. This net charge is reduced in value from that found for (C) in CH_3F solely by the transfer of charge from the compressed (H) fragments in the FCH_3F^- transition state and in $NCCH_3F^-$ by this mechanism and by a transfer of charge from the nucleophile CN^-. The net populations and highly localized charge density contours of the (F) fragments in both transition states clearly indicate the incipient formation of an F^- ion, particularly in the displacement by CN^-. Are these distributions representative of what are called "tight ion pairs?"[12] As discussed below in the section on the energetics of these charge redistributions, it is difficult to rationalize such a near separation of an F^- to yield a single ion pair without the accompanying new bond formation with either solvent or nucleophile.

Partitioning of the Activation Energies

The changes in the energies of the fragments in the formation of the two transition states are listed in Table II. From the sign of the change in the kinetic energy, together with the relationship $\Delta T(A) = -\Delta E(A)$, one can immediately draw the following general conclusions: (a) the nucleophiles F^- and CN^- increase in stability in forming the transition states; (b) the leaving group (F) is considerably destabilized in both transition states; and (c) the (CH_3) fragment is stabilized in both transition states, particularly in the reaction with CN^-.

In the reactant CH_3F, the (F) fragment possesses a net charge of −0.717 e and an energy which is more stable than that of a free, isolated F^- ion by 199 kcal/mol. In the transition state, FCH_3F^-, the net charge on the leaving (F) has developed to −0.864 e and its energy has increased to within 60 kcal/mol of the energy of a free F^- ion. Thus, the process of bond breaking with the leaving group contributes 139 kcal/mol to the energy of activation. The final energy of activation is, however, greatly reduced from this value (to ~7 kcal/mol) by the attendant bond formation with the nucleophile F^-. The nucleophilic (F) fragment is stabilized by the partial bond formation to (CH_3) in the transition state by 60 kcal/mol. In addition, the (CH_3) fragment undergoes a net stabilization (bond formation exceeding bond breaking) of 72 kcal/mol.

(12) R. A. Sneen, *Accounts Chem. Res.*, 6, 46 (1973).

The transition state of the CN^- displacement reaction, in accordance with the Hammond–Polanyi postulate,[13] has a geometry and energy close to those of the products $CH_3CN + F^-$, which possess a higher energy (by 5.24 kcal/mol) than the reactants $CH_3F + CN^-$. The leaving (F) fragment in this reaction has a net charge of −0.954 e and an energy raised to within only 36 kcal/mol of that of a free F^- ion. Thus, bond breaking with the leaving (F) has proceeded to a much further extent in the reaction of CH_3F with CN^- than with F^- and contributes ~163 kcal/mol to the energy of activation in the CN^- reaction. Bond formation with the entering CN^- group stabilizes the transition state by only 22 kcal/mol, the major stabilization arising from the energy decrease experienced by the (CH_3) fragment, by 119 kcal/mol. The (C) of the CN^- is strongly stabilized by the new bond formation to (CH_3) in the transition state, its energy changing by −97 kcal/mol. The increased bonding of (C) of CN^- with (CH_3) decreases the extent of its bonding to the (N) fragment. This effect, as evidenced by the loss of 0.203 electronic charge by (N), results in an energy increase for this fragment of 75 kcal/mol.

The overall energy of activation of 22 kcal/mol for the CN^- reaction is greater than that of the F^- reaction, because of the greater degree of bond breaking relative to bond formation in the former reaction. The very unsymmetrical geometry of the FCH_3CN^- transition state is in accord with the reacting bond rule of Swain and Thornton.[14] If one equates basicity with proton affinity, then, at the Hartree–Fock level, F^- is a stronger base than CN^-.[15] Viewing the reaction as $F^- + CH_3CN$, the transition state should, according to Swain and Thornton, resemble reactants more than products as is predicted here. The ordering of the magnitudes of the activation energies for reactions 6 and 7 would probably be reversed if the reactions were to occur in a polar solvent. The fluoride ion is known to be the most tightly solvated of the singly charged anions. The energy required for its partial desolvation when acting as a nucleophile in reaction 6 would contribute more to the energy of activation than the corresponding effect would for the cyanide ion in reaction 7. Furthermore, since the leaving (F) is more nearly separated as an F^- ion in reaction 7, solvation of this fragment in the transition state would also lower the activation energy of reaction 7 more than that of 6.

In summary, the virial partitioning method demonstrates the importance of the stabilization of the transition state derived from the process of partial bond formation with the nucleophile. This and the associated stabilization of the (CH_3) fragment reduce the destabilization of the system associated with the partial bond breaking with the leaving group.

Reference to Table II indicates that the formation of the transition state results in a stabilizing decrease in the electron–nuclear potential interaction ($\Delta\bar{V}' < 0$) for all the fragments. Aside from the protons, this stabilizing effect is smallest for the leaving (F) fragment

(13) G. S. Hammond, *J. Amer. Chem. Soc.*, 77, 334 (1955); J. Horiuti and M. Polanyi, *Acta Physicochim. USSR*, 2, 505 (1935).

(14) C. G. Swain and E. R. Thornton, *J. Amer. Chem. Soc.*, **84**, 817 (1962).

(15) Using Hartree–Fock values, the energy change for $F^- + H^+ \rightarrow HF$ is *ca.* −387 kcal/mol and for $CN^- + H^+ \rightarrow HCN$ it is −363 kcal/mol.

in both reactions. Every fragment experiences a destabilizing increase in the electron–electron ($\Delta\bar{V}'' > 0$) and nuclear–nuclear ($\Delta\bar{V}_n > 0$) repulsive interactions. The sum of the changes in $\bar{V}'$, $\bar{V}''$, and $\bar{V}_n$ for the approach of two separate, neutral, spherical charge distributions vanishes, for in this case both $\Delta\bar{V}''$ and $\Delta\bar{V}_n$ equal $-0.5\bar{V}'$. Reference to Table II indicates that this pattern of energy changes is a general phenomenon. With the exception of the leaving (F), one finds $\Delta\bar{V}'' \sim \Delta\bar{V}_n$ and both these are *ca.* $-0.5\Delta\bar{V}'$. It is the small (relative to the absolute magnitude of the energies) departure from this balance in the changes of $\bar{V}'$, $\bar{V}''$, and $\bar{V}_n$ which determines whether the attractive or repulsive interactions dominate the energy change for a given fragment and thus determine whether it is stabilized or destabilized in the process.

Because of the motion of the leaving (F) fragment away from its nearest neighbors in the remainder of the system, the magnitude of $\Delta\bar{V}'(\mathrm{F})$ is relatively small. In fact, $\Delta\bar{V}'_{\mathrm{C}}(\mathrm{F})$ and $\Delta\bar{V}'_{\mathrm{H}}(\mathrm{F})$ in reaction 6, the change in the interactions of the carbon and hydrogen nuclei with the charge density in (F), are both greater than zero. $\Delta\bar{V}'_{\mathrm{F}}(\mathrm{F})$, the change in the self-interaction, decreases by only -0.014 au, the major contribution to the decrease in $\bar{V}'(\mathrm{F})$ arising from the new interaction of (F) with the approaching fluorine nucleus of the nucleophile. A similar breakdown for $\Delta\bar{V}'(\mathrm{F})$ is found for reaction 7 with the major decrease resulting from the interaction of (F) with the C and N nuclei of (CN). There are, however, two significant increases in $\bar{V}''(\mathrm{F})$. One is the repulsion of the charge density in (F) by the charge density of the nucleophiles (F) or (CN) and the second is the increase in the self-repulsion of the electrons in (F) because of the increase in its electron population. The result is a relatively large net increase in the repulsive forces exerted on the leaving (F) and thus a decrease in its stability. In contrast, the contributions to $\Delta V'(\mathrm{F})$ for the nucleophilic (F) are all large in magnitude and negative because of the new nuclear–electron interactions. The sole exception is $\Delta V'_{\mathrm{F}}(\mathrm{F})$ which, because of the charge loss from this fragment, has the relatively small positive value of $+0.098$ au. In this case, the nuclear–electron attractive interactions outweigh the repulsive interactions (electrons are transferred out of the nucleophilic fragment) and the nucleophile is stabilized in the transition state relative to the isolated F^- ion.

In summary, we find paralleling behavior for the energy changes of corresponding fragments in both reactions. Relative to the reactants, the leaving group is destabilized and the nucleophile is stabilized as is the (C) fragment at which substitution occurs. The (H) fragments undergo a small but significant destabilization. In both reactions, $\Delta\bar{V}''(\mathrm{H})$ exceeds $|0.5\Delta V'(\mathrm{H})|$ primarily as a result of the compression of the charge density of the (H) fragments referred to earlier.

The $\sim$45 kcal/mol of compressional energy stored in the (H) fragments in the transition state is released as the system proceeds to products. The release of this energy, coupled with further bond formation with the nucleophilic fragment, serves as a driving force for further motion of the system along the specific reaction coordinate. This is a simple example of an important phenomenon and of how it may be determined by the virial partitioning method. One may isolate those spatial regions or fragments of a reacting system in which potential energy is at first accumulated and then later released, either to drive the same reaction to completion or to initiate a subsequent one. The ability to spatially identify the "energy rich" regions of a molecular system has obvious applications to the study of enzyme mechanisms.

Secondary Deuterium Isotope Effects in Solvolysis of Cyclopentyl *p*-Bromobenzenesulfonate. Stereochemistry of E1 and SN1 Reactions[1]

Krešimir Humski,* Vahid Sendijarević, and Vernon J. Shiner, Jr.

Contribution from the "Ruder Bošković" Institute, 41000 Zagreb, Croatia, Yugoslavia, Faculty of Technology, University of Zagreb, 44000 Sisak, Croatia, Yugoslavia, and the Department of Chemistry, Indiana University, Bloomington, Indiana 47401. *Received June 7, 1973*

Abstract: Secondary α- and β-isotope effects in solvolysis of cyclopentyl-*1-d*, *cis*-cyclopentyl-*2-d*, *trans*-cyclopentyl-*2-d*, and cyclopentyl-*2,2,5,5-d*$_4$ brosylates were measured in different ethanol–water (E–W) and trifluoroethanol–water (TFE–W) mixtures. The magnitude of the effects indicates that in the E–W mixtures the products are derived by rate-determining substitution and elimination on the reversibly formed intimate ion pair. However, the change to TFE–W mixtures causes a change in mechanism; in these solvents the formation of the solvent separated ion pair is rate determining and the products are formed in fast subsequent attack on this intermediate. Consistent with this interpretation of the isotope effects, the elimination in E–W mixtures was found to be stereospecifically trans, while in TFE–W mixtures it is nonstereospecific. It was also determined that the configuration of the cyclopentanol formed in both types of solvents was inverted in comparison to the starting material. A detailed analysis provides an estimation of the isotope effects in each of the individual steps in the reaction.

Secondary deuterium isotope effects have become a very useful tool for reaction mechanism studies. Thus, the α effect can be used as a criterion for the solvolysis mechanism,[2] and the β effect has been shown to be very sensitive to participation of a neighboring group in solvolytic reactions.[3] The combination of secondary isotope effect data with a detailed product study can yield detailed information on a solvolytic reaction mechanism.

There is considerable evidence supplied by Winstein, *et al.*,[4] that at least three different carbonium ion type intermediates are involved in solvolytic substitution reactions. They are depicted as the tight (or intimate) ion pair, the solvent separated ion pair, and the free ion as indicated in Scheme I. Each of the steps from

Scheme I

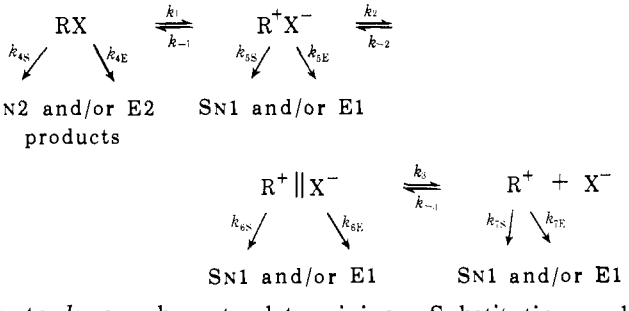

k_1 to k_7 can be rate determining. Substitution and elimination products can be derived from each of the intermediates in SN1 or E1 processes. It is assumed that products are formed irreversibly from the above intermediates and that no additional intermediates are involved. It is also assumed that the products are stable and that processes k_4 to k_7 are irreversible under reaction conditions favorable to substitution and elimination. Substitution and elimination products can be derived either from the same intermediate or from different intermediates. (It seems that the elimination may sometimes occur at an earlier stage of the reaction than substitution.[5])

Recent results show that the α effect is a function of the leaving group as well as of the mechanism.[6] Thus, it was found that for SN1 reactions the upper limit for the α effect (k_H/k_D) is 1.09 for iodides, 1.15 for chlorides, and 1.22 for sulfonate esters. This upper limit is characteristic of a particular leaving group and is fairly independent of changes in solvent polarity and nucleophilicity or substrate reactivity. It was concluded that these large effects are obtained when k_2 is the rate-determining step (conversion from the tight ion pair to the solvent separated ion pair).

Secondary β effects have been shown to be remarkably independent of changes in solvent composition when the quantity of the elimination product is constant.[7] The ratio k_{CH_3}/k_{CD_3} was 1.22 in the solvolysis of 1-phenylethyl chloride in ethanol–water mixtures ranging from 50 to 80 vol % of ethanol and in 97 wt % TFE–W. The yield of styrene was 1 to 3%. It was also found that the magnitude of the β effect may change when the quantity of the elimination product changes with the change of solvent[8] or the leaving group.[9]

Recently the results of solvolysis of 1,2-dimethyl-*exo*-2-norbornyl-*3,3-d*$_2$ *p*-nitrobenzoate in dioxane–water mixtures were published.[10] The isotope effect,

(1) This work was supported in part by the Research Council of Croatia, in part by a PL 480 grant administered by the National Institutes of Health, Bethesda, Md., Agreement No. 02-001-1, and in part by NSF Grant GP 32854.

(2) V. J. Shiner, Jr., "Isotope Effects in Chemical Reactions," C. J. Collins and N. S. Bowman, Ed., Van Nostrand Reinhold, New York, N. Y., 1970, Chapter 2.

(3) D. E. Sunko and S. Borčić, ref 2, Chapter 3.

(4) S. Winstein, B. Appel, R. Baker, and A. Diaz, *Chem. Soc., Spec. Publ.*, No. 19, 109 (1965).

(5) H. L. Goering and K. Humski, *J. Amer. Chem. Soc.*, 90, 6213 (1968).

(6) V. J. Shiner, Jr., and W. Dowd, *J. Amer. Chem. Soc.*, 93, 1029 (1971); V. J. Shiner, Jr., M. W. Rapp, E. A. Halevi, and M. Wolfsberg, *ibid.*, 90, 7171 (1968).

(7) V. J. Shiner, Jr., W. E. Buddenbaum, B. L. Murr, and G. Lamaty, *J. Amer. Chem. Soc.*, 90, 418 (1968).

(8) V. J. Shiner, Jr., W. Dowd, R. D. Fisher, S. R. Hartshorn, M. A. Kessick, L. Milakofsky, and M. W. Rapp, *J. Amer. Chem. Soc.*, 91, 4838 (1969).

(9) S. G. Smith and D. J. W. Goon, *J. Org. Chem.*, 34, 3127 (1969).

(10) K. Humski, *Croat. Chem. Acta*, 42, 501 (1970).